Crystallization Mechanism and Removal of Mixed Solution in Drainage System of Dolomite Tunnel

Junying Rao
Guizhou university
Yanghao Xue (xueyhoffice@163.com)
Guizhou university
Yonghu Tao
Guizhou university

Article

Keywords: Drainage system, Mixed solutions, Crystallization mechanism, Indoor model test, Breaking crystallization

Posted Date: May 31st, 2022

DOI: https://doi.org/10.21203/rs.3.rs-1656620/v1

Crystallization Mechanism and Removal of Mixed Solution in Drainage System of Dolomite Tunnel

Junying Rao[*a]; Yanghao Xue[*b]; Yonghu Tao[*a]

a.Space Structure Research Center(SSRC) of Guizhou University, Guiyang;

b.College of Civil Engineering, Guizhou University, Guiyang.

First author: Junying Rao , Ph.D., jyrao@gzu.edu.cn.

Co-corresponding author: Yanghao Xue, M.Eng, xueyhoffice@163.com.; Yonghu Tao , M.Eng, 1562521808@qq.com.

Abstract: In the construction of tunnels located in the dolomite area, the problems caused by the blockage of the drain pipe (ditch) crystallize one after another. The blockage of the drain pipe (ditch) is one of the potential factors for the leakage of water in the tunnel. Therefore, it is of great engineering significance to find out the factors and mechanisms of crystallization of the dolomite tunnel drainage system. In this paper, the crystallization mechanism and crystal characteristics of the mixed solution of dolomite tunnel drainage system are analyzed based on geological investigation, water quality testing, crystal structure, etc., the causes of crystalline blockage of drainage pipes are analyzed by combining indoor model tests and crystallization breaking tests, and finally, the optimization suggestions of the drainage system are proposed. The results show that the water samples of the dolomite tunnel drainage pipeline belong to the mixed solution of multi-ions, the cations are Ca^{2+}, Mg^{2}+, Al^{3+}, etc., and the anions are CO_3^{2-}、HCO_3^{-}、SO_4^{2-}, etc. Among them, the mass fraction and concentration of Ca^{2+}, Mg^{2+}, Al^{3+} are relatively high. , while the mass fraction and concentration range of Fe^{3+}、Cu^{2+}、Zn^{2+}、Ba^{2+} are approximately 0; the crystal powder contains Cl, O, S, K, Ca, Mg, Al, Na and other elements, and the content of Ca, Mg, Al In comparison, Ca is more, Al is less, and Mg is between the two; after the

evaluation of the degree of crystallization blockage, it is found that the degree of blockage of the transverse drain pipe per linear meter is higher, the circular drainage pipe is lower, and the longitudinal pipe is between the two. The crystal removal effect is more significant with the increase of the ultrasonic vibration frequency. It is found that the optimal removal frequency is 50 kHz, and the optimization suggestion of the drainage system is given in combination with the "V"-shaped pipeline arrangement.

Keyword: Drainage system; Mixed solutions; Crystallization mechanism; Indoor model test; Breaking crystallization

1 introduction

In recent years, with the continuous development of my country's economy, the construction of transportation infrastructure has become an important link. In Guizhou, Sichuan, and other regions in my country, tunnel engineering is one of the key projects, but a series of diseases often occur in the tunnel drainage system, such as blockage and water leakage. etc., which are related to tunnel design and construction [1]. How to effectively prevent tunnel diseases, improve road operation safety, and prolong tunnel life have become hot research topics today.

However, at present, the center of gravity of tunnel design and construction is often too inclined to intuitive factors such as the stability of surrounding rock and the safety of lining; on the contrary, indirect factors such as the service life of the drainage system "hidden" behind the lining are often easily ignored. Water seepage is a common disease in the field of tunnels[2], because water seepage is closely related to the crystallization blockage of the drainage system. The main manifestations are: when the pipeline is blocked, it will lead to an increase in the accumulation of water behind the lining[3], which will increase the water pressure on the lining. When the water pressure exceeds When the ultimate bearing capacity of

the tunnel lining structure is exceeded, the lining structure is easy to crack, which induces water leakage; After the surrounding rock is eroded or softened by flowing water, the strength is reduced and the bearing capacity is weakened, which leads to an increase in the pressure of the lining structure, and even causes the lining structure to crack and cause water leakage. Fig. 1 shows the crystallization of a tunnel drainage system leading to blockage.

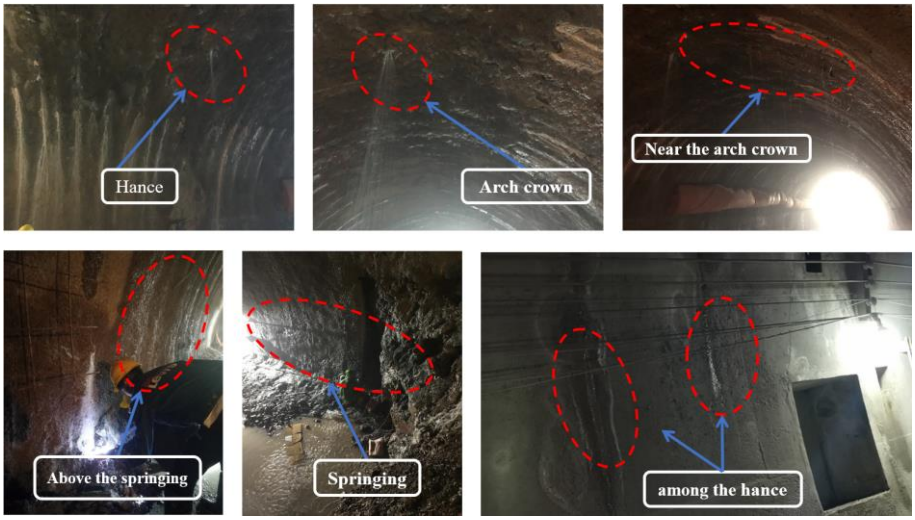

(a) Lining leaks

(b) Crystal overflow

(c) Lining cracking

Fig 1 Crystallization hazards of a tunnel

In the tunnel drainage system in the dolomite area, crystallization often occurs. The initial crystallization time of the tunnel drainage system occurs not only after the tunnel is put into operation, but also during the construction period of some tunnels. Fig. 2 shows the crystallization phenomenon of the Circular drainage pipe outlet, Longitudinal drain pipe, and Transverse Drain pipe of the drainage system of Baiyanjiao Tunnel under construction.

Fig. 2 Crystal blockage of a tunnel drainage system

Through research, problems such as unknown chemical composition of pipeline crystals, unclear microstructure characteristics, unclear crystallization mechanism, and poor crystal breaking effect can be effectively resolved; The mechanism of crystal plugging can be identified and the properties of crystals can be identified, which provides a theoretical basis for solving engineering problems such as crystallization of dolomite tunnel drainage pipes, assists in controlling the stubborn water leakage in tunnels, improves tunnel operation safety, and reduces tunnel maintenance costs.

The phenomenon of karst caves often appears after water erosion in the dolomite area, which belongs to special unfavorable geology. In the field of tunnel engineering, there have been many literatures on the study of karst caves[4,5,6], the construction of projects in this area is not only large in investment, but also restricted by technology and geology. Therefore, it is particularly important to explore the properties of dolomite projects.

It was found that Tao analyzed the characteristics of dolomite and found that dolomite contains CaO, MgO, Al_2O_3, etc.[7]; Xie et al. conducted experiments to study the composition of dolomite and found that the main component of dolomite is $CaCO_3$, and contains MgO, Al_2O_3 and other substances, which have a great impact on the physical and mechanical properties of dolomite[8,9]; Guo analyzed the mechanism of pipeline blockage and found that $Ca(OH)_2$ is easily soluble in groundwater, and it is easy to generate crystals such as $CaCO_3$, which cause the drain pipe to block.[10]; Eichinger et al. analyzed the factors of pipeline blockage, and mainly studied the effect of $CaCO_3$ on pipeline blockage, the study showed that a small amount of ettringite would be precipitated in a high pH value and saturated solution [11]; Zhang analyzed the mechanism and crystal characteristics of pipeline clogging, and found that pipeline clogging is not only related to the formation of precipitation due to the interaction of various ions, but also to factors such as geology, climate, and design[12,13]; Liu et al. analyzed the tunnel erosion

82 failure mechanism and property characteristics of salt-bearing strata of different rocks and found that
83 soluble salt rocks such as gypsum and Glauber's salt are the material basis for corrosion and expansion.
84 The lining undergoes corrosion, branching, expansion, and extrusion, resulting in damage to the
85 supporting structure[14,15]; Eichinger et al. studied pipeline blockage caused by $CaCO_3$ precipitation and
86 found that its hydrochemistry principle mainly includes cement slurry dissolution and solution mixing,
87 and calcium carbonate will grow to various degrees[16]; Girmscheid et al. analyzed the mechanism of
88 pipeline blockage and found that there may be lime in the pipeline interacting with atmospheric
89 conditions to form calcite, causing a blockage[17,18].

90 Ye investigated the crystal blockage of a tunnel under construction and found that more carbonates
91 in the groundwater will make crystals more likely to be formed in the drainage pipe of the tunnel. The
92 solution ion concentration and crystal accumulation capacity in the drainage pipe is Important factors
93 affecting the generation of blockages in drains[19]; When Jung et al. studied the factors of pipeline
94 blockage, they found that the precipitates were mainly caused by the deterioration of concrete and the
95 chemical reaction between ions in the pipe[20]; Park et al. analyzed the relationship between pipeline
96 deterioration and blockage and found that blockage could easily lead to tunnel aging and deterioration.
97 Through experiments, it was found that the slope of the drainage pipe had a great relationship with the
98 blockage[21]; Liu et al. studied the anti-crystallization analysis of flocking at different flow rates through
99 model tests, and found that flocking can effectively inhibit the growth of crystals, but this technology is
100 difficult to operate, especially in practical tunnels, and it is not easy to achieve[22]; Zhou believes that
101 adding carbonic anhydrase or high-efficiency scale inhibitor to the tunnel drainage pipe can inhibit the
102 precipitation of precipitated crystals in the drainage pipe, thereby delaying the blockage process, but this
103 method can only cure the symptoms but not the root cause[23].

To sum up, it is found that the crystal composition in the dolomite tunnel drainage pipeline system: in addition to $CaCO_3$, there are oxides such as MgO and Al_2O_3, and the precipitated crystals of the solution after dissolution are complex, so the crystal composition in the drainage pipeline needs to be clarified; In addition, the solution in the dolomite tunnel is a multi-ion mixed solution, and its precipitation is not only one of $CaCO_3$, and the mixing ratio of different ion concentrations not only affects the crystallization formation mechanism, but also determines the properties of crystals, and the crystallization law of the pipeline is not clear; Finally, in terms of crystal removal, the chemical method may cause damage to the surrounding environment, the mechanical method and tube flocking method are difficult to operate, the scale inhibitor method does not cure the root cause, and there are some limitations in such methods, so crystal removal countermeasures are still necessary. In this paper, the crystallization blockage of the dolomite tunnel drainage system is taken as the breakthrough point to explore the composition and crystallization mechanism of the mixed solution of the dolomite drainage system. Combined with laboratory tests and existing research results, the countermeasures and suggestions for solving the crystallization blockage of the dolomite drainage pipeline system are finally given.

2 Crystal composition analysis

This section investigated the crystallization of many tunnels, such as Xiaowan Tunnel, Dahe Interchange Tunnel, Xindianzi Tunnel, and Baiyanjiao Tunnel (hereinafter referred to as tunnels A, B, C, and D), collected water samples and crystalline powder, and numbered them. Combined with SEM, XRD, and EDS analysis, the water quality and crystalline composition of tunnel drainage pipes in the dolomite area were verified.

2.1 Geological survey

This section's geological survey relies on the project tunnel as an example, the scene as shown in Fig. 3, the tunnel area is mainly dolomite, with limestone, and clastic soil.

Fig. 3 Field investigation of tunnel

Aiming at the problem of crystallization blockage in the dolomite tunnel, the crystallization of the tunnel drainage pipe in the dolomite area is analyzed by field investigation, photograph, and water quality sampling, as shown in Fig. 4. The crystallization blockage of drainage pipes in some tunnels is shown in Fig. 5.

Fig. 4 Crystallized powder and water sample

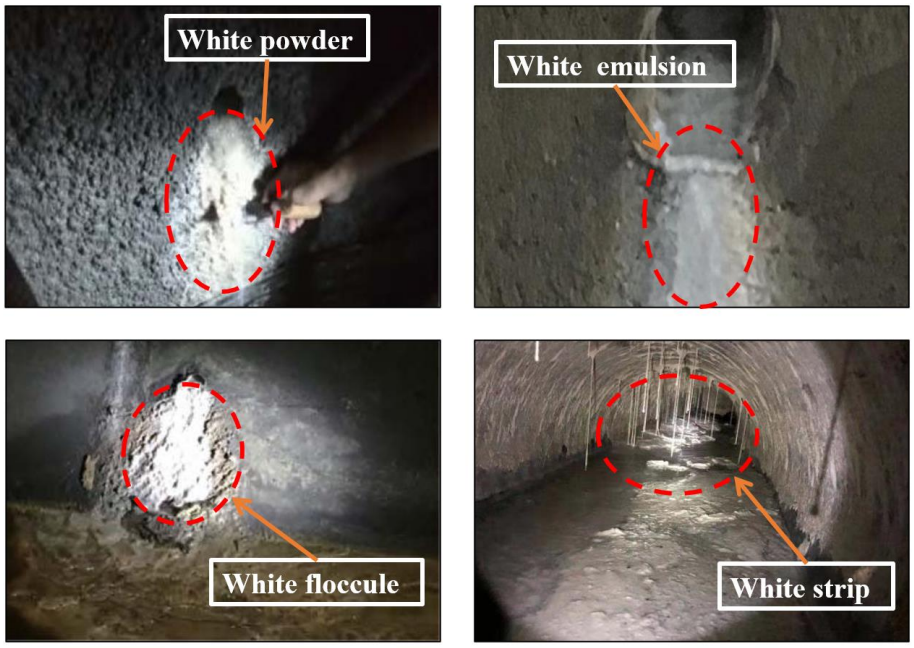

Fig. 5 Crystal blockage of tunnel drainage pipe

According to the on-site investigation, dolomite is carbonate salt, which is easy to dissolve, and its main component is calcite, which is widely distributed in Sichuan, Guizhou, and other places. Because dolomite has the characteristics of easy dissolution, the bubbles generated by the contact of dolomite with weak hydrochloric acid will easily lead to crystal blockage in the tunnel drainage pipe. In addition, the investigation also found that there are many crystals at the outlet of the Transverse drain pipe and the Longitudinal drain pipe, and there are few crystals in the Circular drainage pipe.

The preliminary analysis shows that the dolomite is easily dissolved under the action of groundwater scouring, and the groundwater has the effect of dissolution and seepage. When groundwater moves, it will carry a lot of debris, slag, particles, etc. into the pipeline and accumulate, and the accumulation will increase with time, thus causing the tunnel drainage pipe to be blocked; With the change of temperature and precipitation, due to the supplement or loss of groundwater, the concentration of ions in groundwater changes, which affects the crystallization; Microbial factors [24,25] and plant factors also affect the CO_2 content in the surrounding rock and the plasma concentrations of Ca^{2+}, Mg^{2+}, and Al^{3+}, as shown in Fig.

6 and Fig. 7.

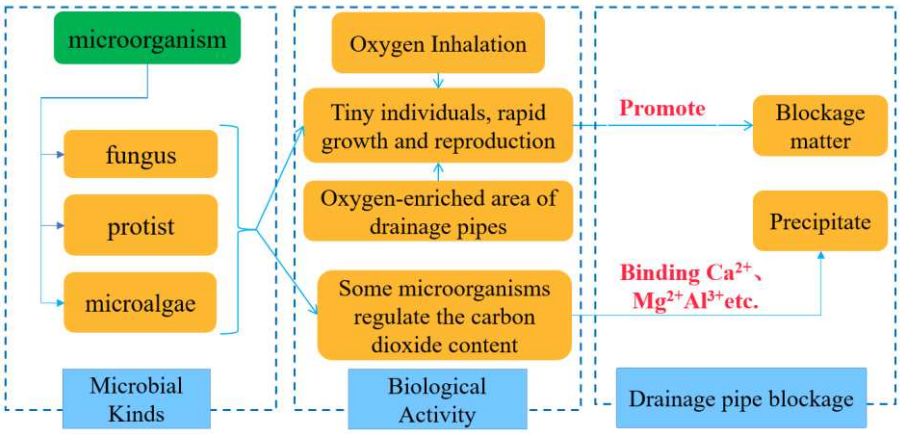

Fig. 6 Microbial crystal plugging

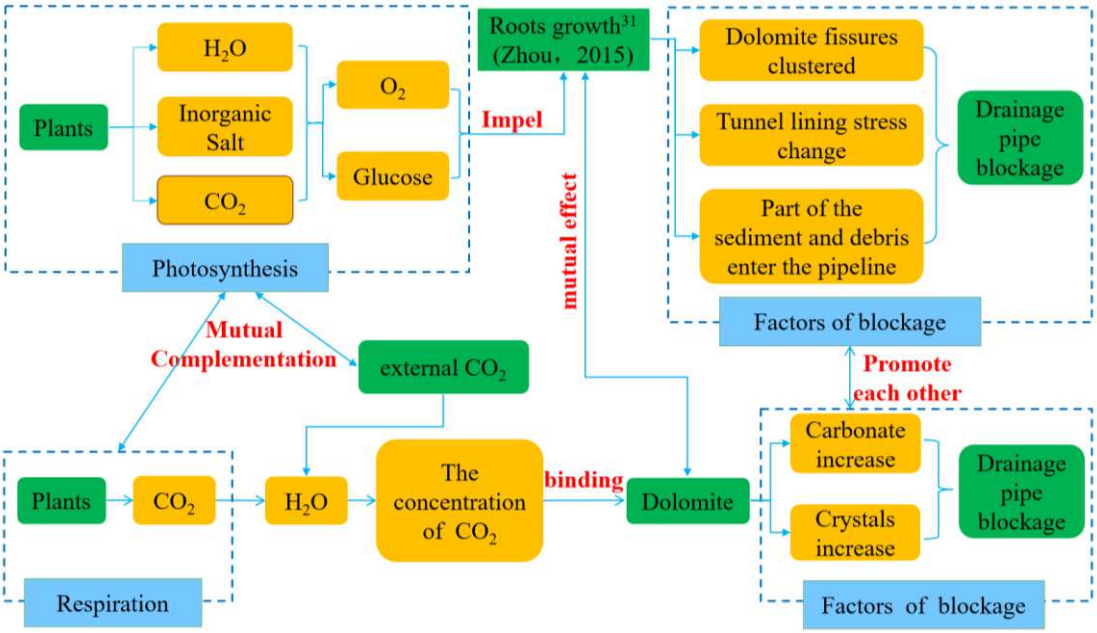

Fig. 7 Clogging caused by plant factor crystallization

2.2 Analysis of water quality composition

The water samples from the tunnel drainage pipes were filtered and allowed to stand for water quality analysis, as shown in Fig. 8.

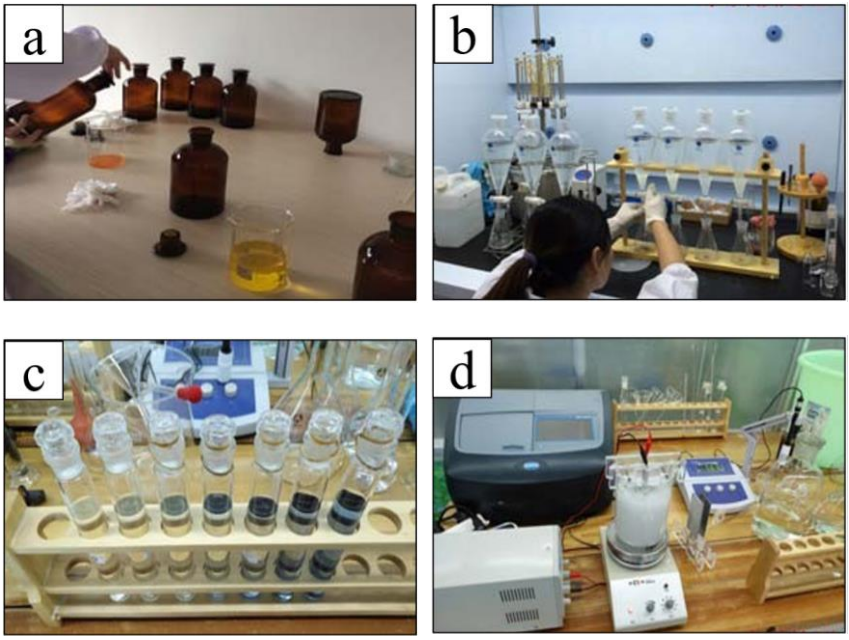

(a) Cleaning equipment (b) Sample preprocessing

(c) Sample grading (d) Examination of water quality

Fig. 8 Example of water quality inspection process

For the convenience of analysis, the crystalline powder and water samples collected on site are numbered, and the crystalline powder on the left and right of the A tunnel is marked as A1 and A2 respectively, and the left and right water samples of the A tunnel are marked as A3 and A4 respectively. Tunnels B, C, and D are marked in the same way, as shown in Fig. 9.

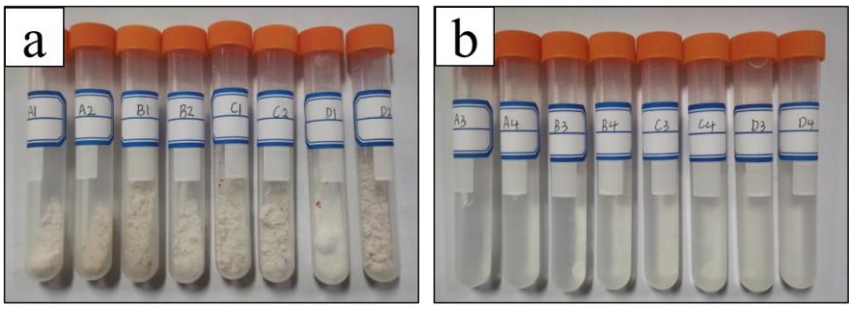

(a) Crystallized powder (b) Crystallized water samples

Fig. 9 Sampling number

According to the results of water quality analysis, all kinds of ions, ion concentration range, and mass percentage content were counted, and the ion statistics are shown in Table 1.

Table 1 Statistics of relevant ion indicators

Numbering	Ion	Density range /g.cm^{-3}	Concentration range /mg.L^{-1}	Mass fraction range/%
1	CO_3^{2-}	1.458～13.378	0.074～0.152	23.47%～28.82%
2	SO_4^{2-}	3.493～54.287	0.051～0.058	12.69%～22.55%
3	Ca^{2+}	0.741～52.266	0.028～0.189	10.79%～19.43%
4	Mg^{2+}	0.053～0.449	0.002～0.014	0.58%～0.85%
5	Na^{+}	2.552～7.974	0.059～0.335	19.82%～22.88%
6	Al^{3+}	0.035～0.765	0.002～0.028	0.58%～1.96%
7	K^{+}	0.999～18.550	0.020～0.175	7.56%～17.53%
8	Cl^{-}	0.015～0.043	0.015～0.043	3.96%～5.95%
9	Fe^{3+}	0.030～0.050	0.000～0.000	0.13%～0.19%
10	Cu^{2+}	0.0001～0.002	0.000～0.000	0.05%～0.050%
11	Zn^{2+}	0.0007～0.002	0.000～0.000	0.05%～0.051%
12	Ba^{2+}	0.00007～0.0029	0.000～0.000	0.00%～28.93%

Table 1 shows that the dolomite tunnel crystal sample is a complex mixture, is a multi-ion mixed solution, containing cations: Ca^{2+}、Mg^{2+}、Fe^{3+}, anions: SO_4^{2-}、CO_3^{2-} etc. A series of complex physical and chemical reactions form crystallization blocking pipes, so it is necessary to study the composition of crystals. To facilitate the later analysis, the ion classification is as follows : (1) Crystalline ions, refers to the ion itself that is easy to combine with other ions to form crystalline precipitation ions, such as Ca^{2+}、

Mg^{2+}、SO_4^{2-}、CO_3^{2-}、Al^{3+}; (2) Non-crystalline ions, refer to the ion itself is not easy to crystallize with other ions to form precipitation blockage, such as Cl^-、K^+、Na^+.

3 Crystal microstructure analysis

The literature shows that the energy peak diagram of each element can be obtained by the phase analysis method, the crystal structure and shape can be understood from the microscopic point of view, and the element content and shape characteristics in different regions can be obtained[26,27]. XRD can use the wavelength corresponding to the X-ray diffraction peak to reversely deduce the crystal seed of the crystal and determine the material composition.

3.1 Phase analysis

Scanning electron microscopy (SEM) was performed on the crystals sampled at the site, and the scanning results are shown in Fig. 10.

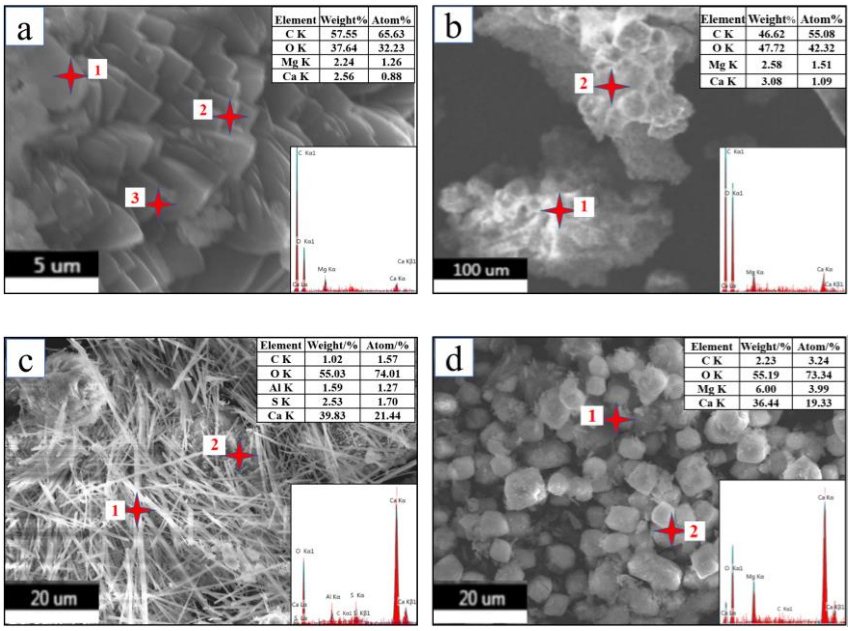

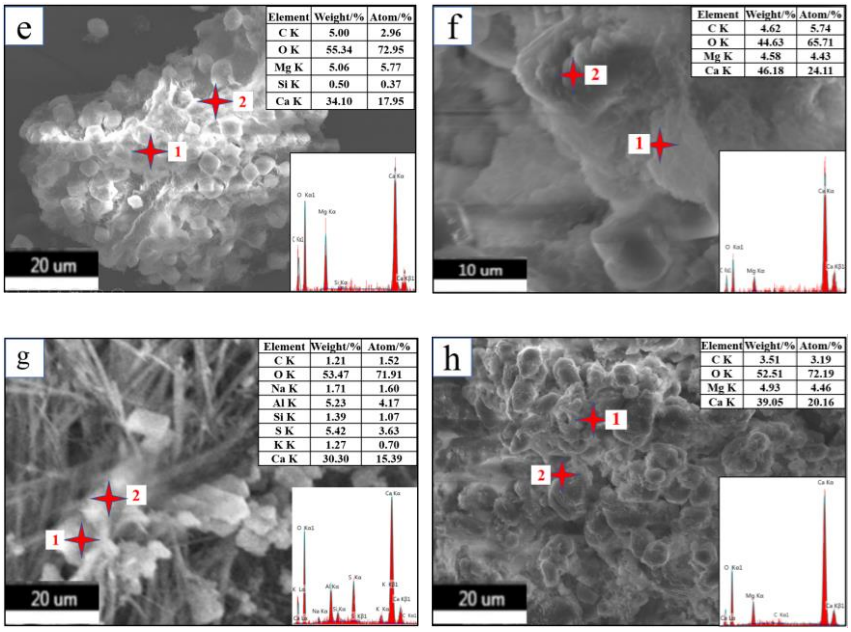

(a)A1 sample; (b)A2 sample; (c) B1 sample;(d) B2 sample

(e)C1 sample; (f)C2 sample; (g) D1 sample; (h) D2 sample

Fig. 10 SEM analysis

Fig. 10 (a) shows that: magnesium as a whole is a white thin block, granular accumulation into rows, the structure is close and complete, Ca element presents coarse wedge; Fig. 10 (b) shows that the whole magnesium is bright white granular, multi-granular accumulation forming, the structure is close and complete, calcium is dark white a coarse granular; Fig. 10 (c) shows that: calcium presents white coarse silk, widely distributed, aluminum as a whole presents bright white fine silk, loose structure; Fig. 10 (d) shows that part of magnesium as a whole is bright white granular, granular accumulation, coarse calcium particles, dark; Fig. 10 (e) shows that : magnesium as a whole is bright white granular, granular accumulation forming, compact structure, and calcium presents bulky; Fig. 10 (f) shows that: magnesium as a whole is a white fine block, calcium presents a dark coarse block; Fig. 10 (g) shows that aluminum as a whole is a bright white fine block, calcium bulky accumulation. In addition, from Fig. 10 (a), which comes from the early completed lining, the overall microstructure is massive, and the

crystals are closely contacted. From Fig. 10 (d), which comes from the drainage pipe wall, the particle boundary is clear, the overall microstructure is granular, and there are many voids between crystals. From Fig. 10 (h), which comes from the recently completed shotcrete, the overall microstructure is between (a) and (d), and the crystals still have granular characteristics, but the voids between particles are partially connected and the boundary of particles is blurred. This can explain the crystal blockage to a certain extent: the crystal is formed by the accumulation of small particles, and the contact of small particles is not reliable, so it is easy to be transferred to other places by water. When the particles gradually accumulate somewhere, the accumulation amount increases with time, and the ca + in water is continuously supplemented. The contact between small particles becomes closer and closer, and the overall microstructure becomes massive. Finally, it is closely attached to the wall or lining and other structures.

3.2 Compositional analysis

EDS analysis was performed on the crystalline powder samples A1, A2, B1, B2, C1, C2, D1, and D2 sampled in the field, and the elements are shown in Fig. 11.

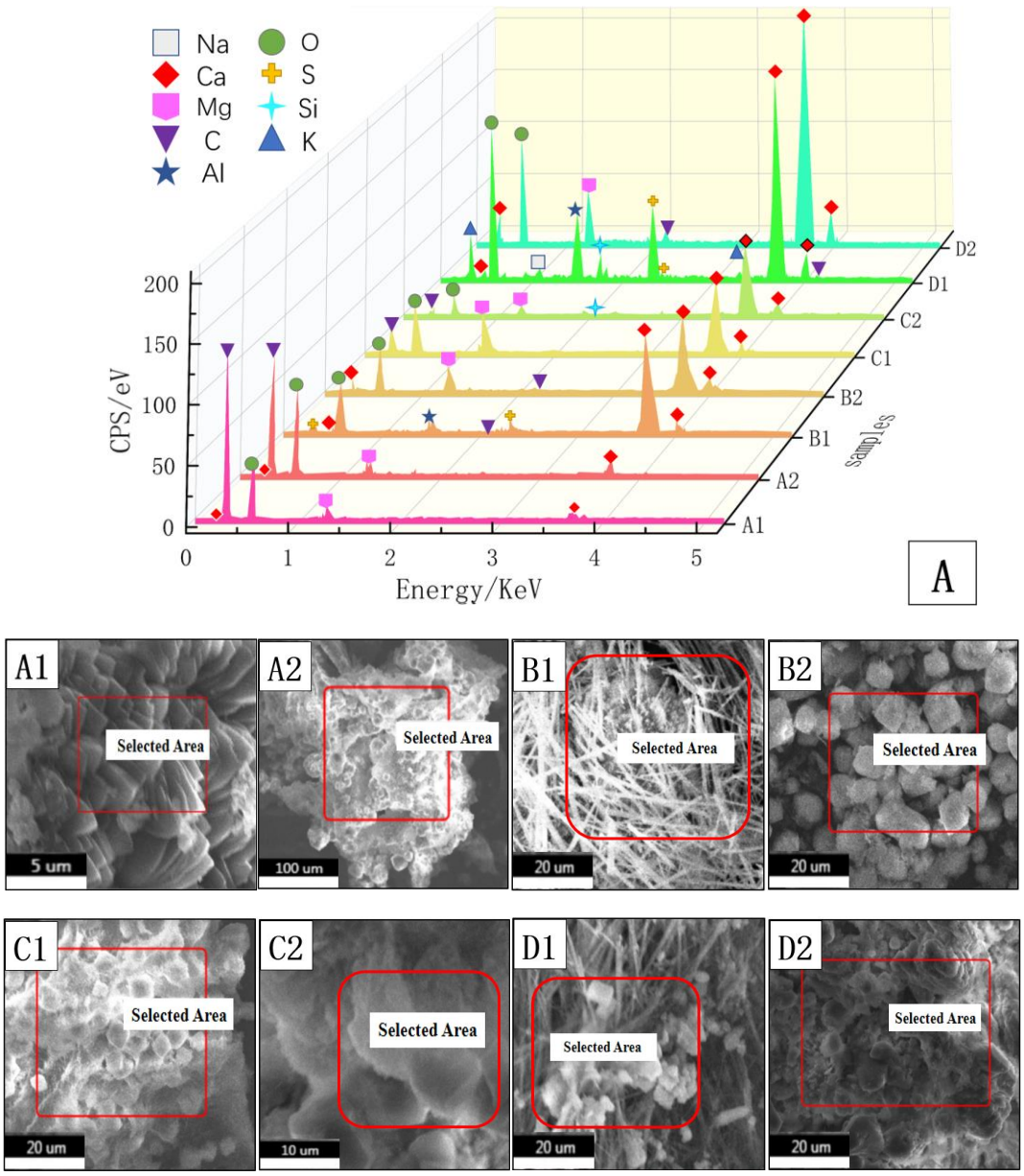

Regions A1, A2, B1, B2, C1, C2, D1, D2 for each sample in A

Fig. 11 EDS analysis

According to EDS analysis results, the main elements are: Na, Ca, Al, C, Mg, K, Si, O, and S; crystalline ions contain Ca^{2+}、Mg^{2+}、Al^{3+}etc. ; In general, the energy peak of calcium is relatively high, indicating that its content is also relatively high, followed by the content of Mg and Al. Therefore, the influence of Mg and Al on crystallization cannot be ignored in the study. Due to the existence of C, S, O and other elements, CO_3^{2-} and OH^- are easy to occur in water, and then $Mg(OH)_2$ and $Al(OH)_3$, and other

precipitates are easy to produce, which will affect the drainage pipeline. Fig. 11 also verifies the ion species in water quality analysis.

Although EDS analysis can effectively determine the elements in the formulation area, H and HE cannot be determined according to the position of the characteristic spectral line. Since the properties of the He element are relatively stable and it is difficult to form compounds, the influence of this element is not considered. In the XRD analysis, the phase analysis with and without the H element can be carried out based on Jade 6.5 software to make up for the deficiency of EDS analysis, as shown in Fig. 12.

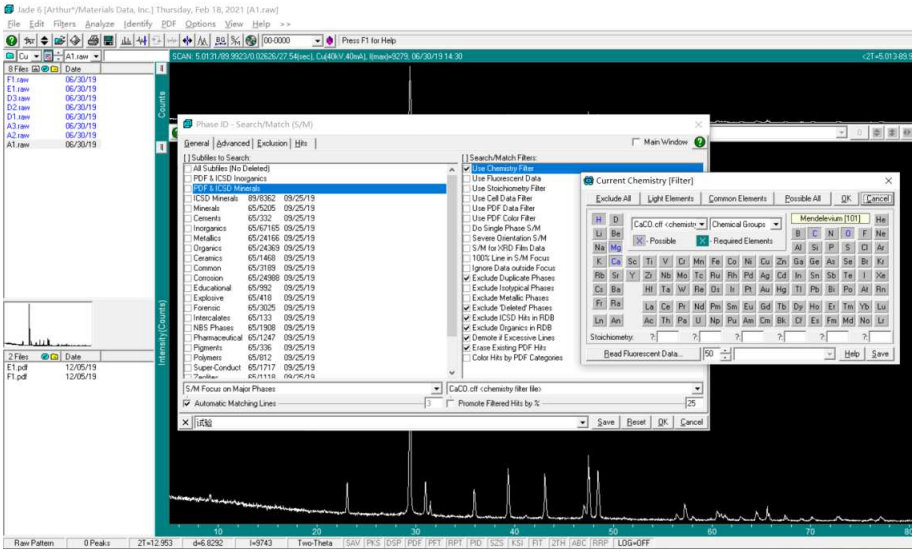

Fig. 12 H element screening

XRD test was used to analyze the crystalline composition of the dolomite tunnel drainage system, as shown in Fig. 13.

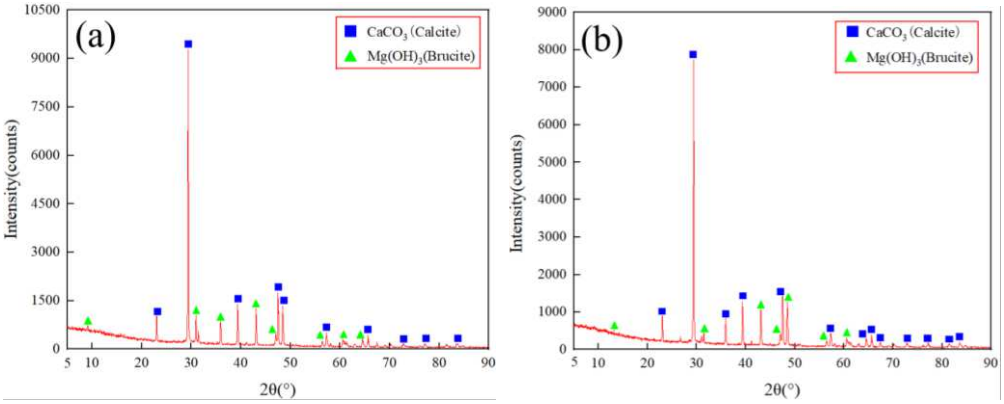

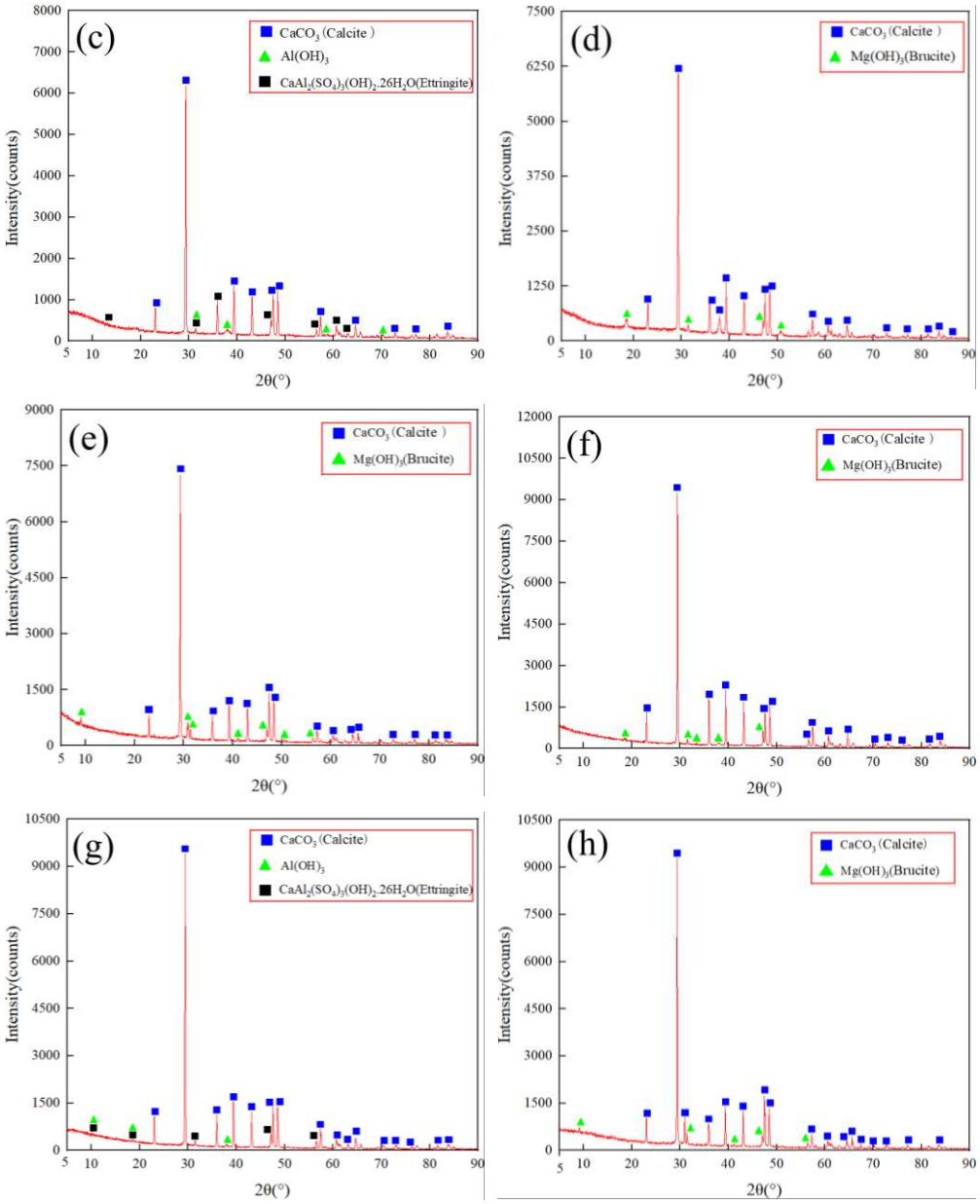

(a) is XRD of Sample A1; (b) is XRD of Sample A2; (c) is XRD of Sample B1;

(d) is XRD of Sample B2; (e) is XRD of Sample C1; (f) is XRD of Sample C2;

(g) is XRD of Sample D1; (h) is XRD of Sample D2.

Fig. 13 XRD analysis

Fig. 13 shows that: Fig. 13 (a), Fig. 13 (b), Fig. 13 (d), Fig. 13 (e), Fig. 13 (f), and Fig. 13 (h) show that in the crystalline powder, in addition to $CaCO_3$, also contains part of $Mg(OH)_2$; Fig. 13 (c), Fig. 13 (g) shows that in addition to $CaCO_3$, $Mg(OH)_2$, there are some $Al(OH)_2$, ettringite coexist

in the crystalline powder.

In summary, it is found that the crystalline powder contains Cl, O, S, K, Ca, Mg, Al, Na, and other elements, combined with H in water and C in air. In nature, these elements generally exist in the form of ions or compounds, namely: Cl^-, O^{2-}, SO_4^{2-}, K^+, Ca^+, Mg^{2+}, Al^{3+}, Na^+, OH^-, H^+, CO_3^{2-}plasmas, which combine to form new substances, such as $Mg(OH)_2$, $CaCO_3$, $Al(OH)_3$, etc. Crystallization precipitation, coupled with the accumulation of some physical debris plugs, and then pipeline crystallization plugs; caCO3 has the highest content, but it also contains non-negligible blockages such as $Mg(OH)_2$, $Al(OH)_3$.

Comprehensive EDS, XRD, SEM analysis, and different elements combined to form crystalline precipitation, resulting in different wall adhesions, blockage degree, and crystalline blockage as shown in Fig. 14.

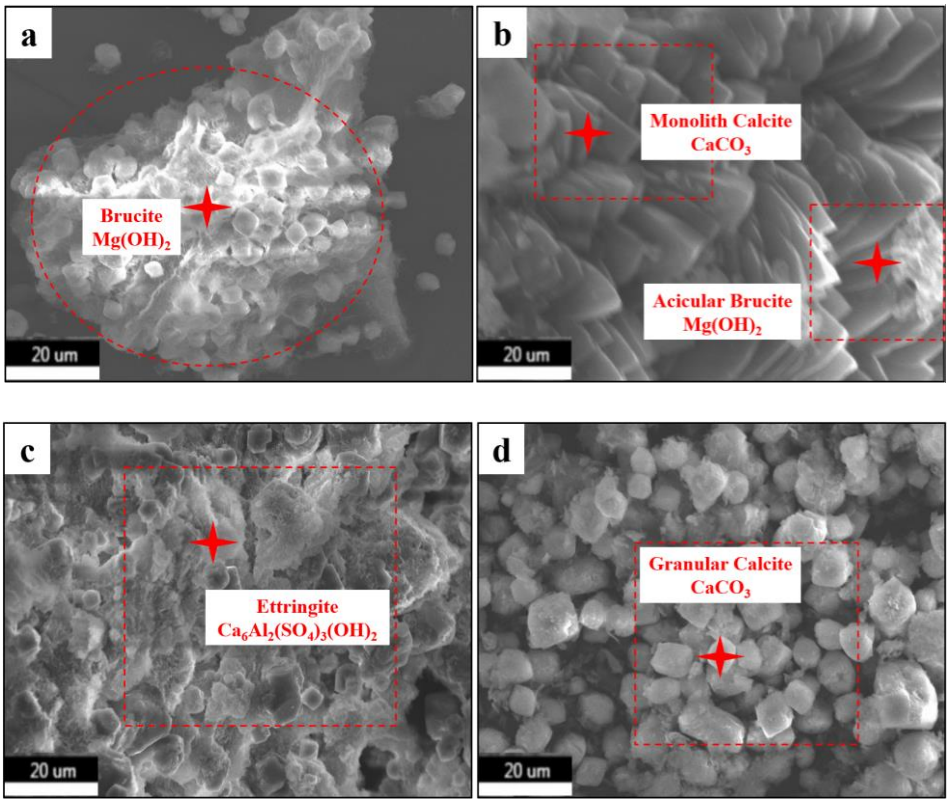

Fig. 14 Crystal structures of some compounds

Fig. 14 shows that the microstructure of crystals is different, and the main structural difference

268 depends on the corresponding crystalline ions, such as the microstructure of $Mg(OH)_2$ depends on the
269 microstructure of Mg element, the microstructure of $CaCO_3$ depends on the microstructure of Ca element,
270 the microstructure of $CaAl_2(SO_4)_3(OH)_2 \cdot 26H_2O$ depends on the microstructure of Ca element and Al
271 element.

272 Combined with EDS, SEM, and XRD analysis, it is found that calcium content is more, magnesium
273 content is second, and aluminum content is less in crystalline ions. The crystal calcite $CaCO_3$ is white,
274 needle-like, fine-grained, and massive. The crystal $Mg(OH)_2$ is bright white, filamentous, and powder-
275 like. Aluminum and calcium form ettringite $CaAl_2(SO_4)_3(OH)_2 \cdot 26H_2O$ crystal, and there are some milky-
276 white $Al(OH)_3$ crystals, and the structure is stacked.

277 **4 Mechanism of crystal blockage**

278 **4.1 Crystal formation theory**

279 According to Table 1 in Section 2, the water samples of the dolomite tunnel drainage system contain
280 cations such as Ca^{2+}、Mg^{2+}、Na^{+}、K^{+}、Fe^{3+}、Cu^{2+}、Zn^{2+}, and Ba^{2+}, and anions such as CO_3^{2-}、SO_4^{2-}、
281 HCO_3^{-}. According to the interaction between ions, the main reactions may be:

$$HCO_3^{2-} \rightarrow H^{+} + CO_3^{2-} \quad (1)$$

$$HCO_3^{2-} + H^{+} \rightarrow CO_2 \uparrow + H_2O \quad (2)$$

$$Ca^{2+} + CO_3^{2-} \rightarrow CaCO_3 \downarrow \quad (3)$$

$$Ca^{2+} + SO_4^{2-} \rightarrow CaSO_4 \downarrow \quad (4)$$

$$CaSO_4 + CO_3^{2-} \rightarrow CaCO_3 \downarrow + SO_4^{2-} \quad (5)$$

$$Ca^{2+} + 2HCO_3^{-} \rightarrow CaCO_3 \downarrow + CO_2 \uparrow + H_2O \quad (6)$$

$$Mg^{2+} + OH^{-} \rightarrow Mg(OH)_2 \downarrow \quad (7)$$

$$Mg^{2+} + 2HCO_3^- \rightarrow MgCO_3\downarrow + CO_2\uparrow + H_2O \quad (8)$$

$$Mg^{2+} + CO_3^{2-} \rightarrow MgCO_3\downarrow \quad (9)$$

$$MgCO_3 + Ca^{2-} \rightarrow CaCO_3\downarrow + Mg^{2+} \quad (10)$$

$$Al^{3+} + 3OH^- \rightarrow Al(OH)_3\downarrow \quad (11)$$

$$Al^{3+} + 3HCO_3^- \rightarrow Al(OH)_3\downarrow + 3CO_2\uparrow \quad (12)$$

$$Al(OH)_3 + OH^- \rightarrow AlO_2^- + 2H_2O \quad (13)$$

$$Ba^{2+} + CO_3^{2-} \rightarrow BaCO_3\downarrow \quad (14)$$

$$Ba^{2+} + SO_4^{2-} \rightarrow BaSO_4\downarrow \quad (15)$$

$$Ba^{2+} + 2HCO_3^- \rightarrow BaCO_3\downarrow + CO_2\uparrow + H_2O \quad (16)$$

$$Fe^{3+} + 3OH^- \rightarrow Fe(OH)_3\downarrow \quad (17)$$

$$Cu^{2+} + 2OH^- \rightarrow Cu(OH)_2\downarrow \quad (18)$$

$$2Cu^{2+} + 2CaCO_3 + H_2O \rightarrow Cu_2(CO_3)(OH)_2\downarrow + 2CaSO_4\downarrow + CO_2\uparrow \quad (19)$$

282 In the (3) ~ (19) chemical reaction, the type of precipitation is shown in Table 2.

283 Table 2 Types of Precipitation

Kind of precipitation	Color	Chemical property	After hydrolysis	Crystal shape
$CaCO_3$	white	soluble in acid	Alkaline	fibroid
$BaCO_3$	white	soluble in acid	Alkaline	granular
$MgCO_3$	white	sparingly soluble in acid	Alkaline	amorphism
$CaSO_4$	white	sparingly soluble in acid	Alkaline	columnar

$BaSO_4$	white	soluble in acid	Alkaline	Plate crystal type
$Al(OH)_3$	white	soluble in acid and alkali	Alkaline	Single crystal hexagonal flakes
$Fe(OH)_3$	fulvous	soluble in acid	Alkaline	needle-like, fish-scale-like
$Mg(OH)_2$	White, gray	soluble in acid	Alkaline	Leaf - shaped, leaf - shaped
$Cu(OH)_2$	Blue	soluble in acid	Alkaline	floccule
$Cu_2(CO_3)(OH)_2$	green	soluble in acid	Alkaline	Grape-shaped

4.2 Crystallization process

Recrystallization (Secondary nucleation) may occur during crystal formation, This process mainly includes aggregation and breakage[28]. Crystal aggregation refers to the phenomenon that the crystals in nucleation or growth collide, fuse, and separate with other crystals, and some grains stick together to form new grains, and the nuclei grow again. Crystal breakage means that some grains are broken, making the grains smaller and becoming smaller again. The process is shown in Fig. 15.

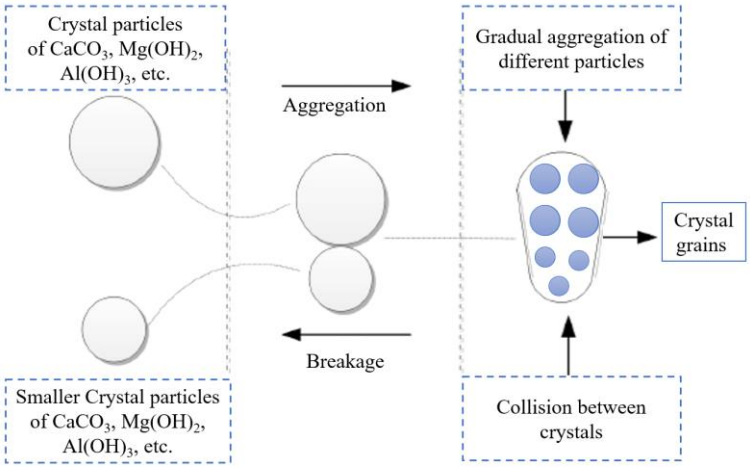

Fig. 15 Crystal aggregation and breakage

4.3 Crystallization mechanism analysis

It can be seen from the third section that the content of Fe^{3+}, Cu^{2+}, and Ba^{2+} is very little by SEM scanning electron microscope, XRD test, and water quality test, which is approximately 0, so it can be ignored in crystal precipitation.

It can be seen from Formula (4.5) that $CaSO_4$ precipitation will eventually transform into $CaCO_3$ precipitation, and then CaSO4 crystals will not precipitate when the reaction is sufficient, while Ca^{2+} and Mg^{2+} will spontaneously react with HCO_3^-, SO_4^{2-} and CO_3^{2-} ions. $Al(OH)_3$ precipitation generated by Al^{3+} is amphoteric and can be dissolved in acid and alkali, while dolomite belongs to carbonate rock. The main chemical composition of dolomite is $CaCO_3$, and hydrolysis is alkaline. Some $Al(OH)_3$ precipitation is dissolved to form meta aluminate, and the other part exists in the form of $Al(OH)_3$.

In summary, it is found that there may be $CaCO_3$, $MgCO_3$, $Al(OH)_3$, $Mg(OH)_2$, and other precipitates in the crystallization type. The crystallization mechanism of some ions is shown in Fig. 16[10], and the crystallization blockage of the drainage pipe is shown in Fig. 17.

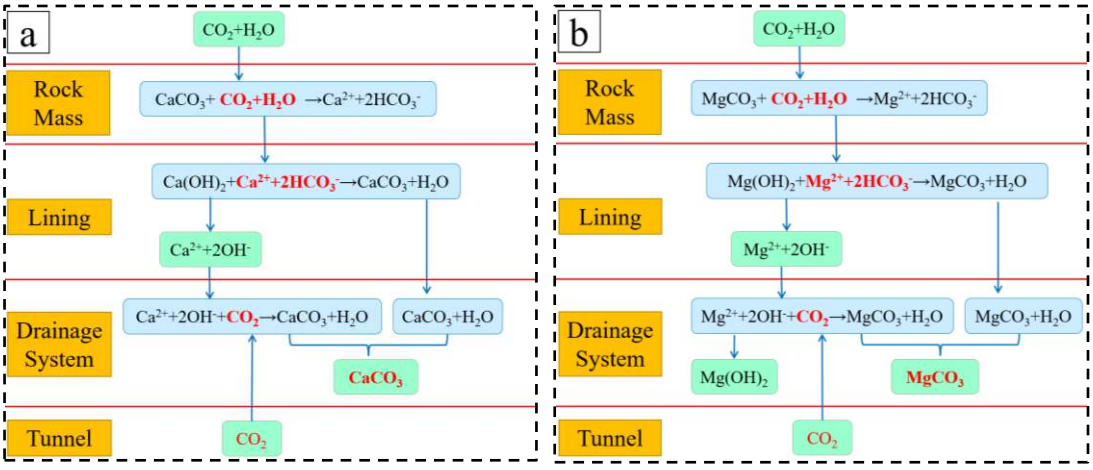

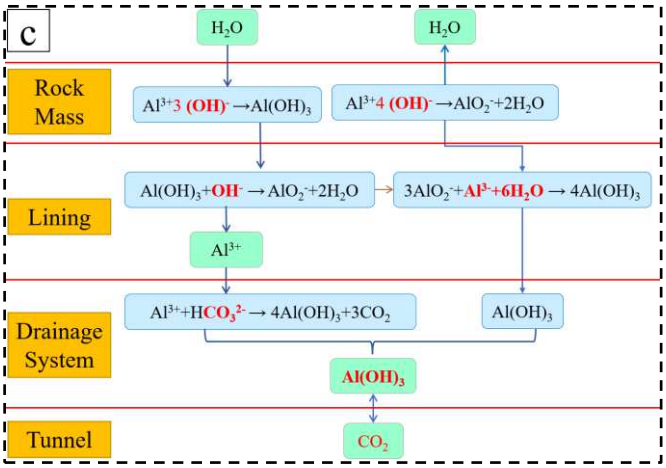

306

307 (a) Ca^{2+} Mechanism of crystal blockage (b) Mg^{2+} Mechanism of crystal blockage

308 (c)Al^{3+} Mechanism of crystal blockage

309 Fig. 16 Mechanism of ion crystallization

310 (a) Ca^{2+} Mechanism of crystal blockage:

311 In the first step: H_2O and CO_2 interact with $CaCO_3$ in the surrounding rock, and the initial products
312 are Ca^{2+} and HCO_3^-; In the second step: Ca^{2+} and HCO_3^- react with $Ca(OH)_2$ in the lining, and gradually
313 produce $CaCO_3$ and H_2O. At the same time, part of $Ca(OH)_2$ in the lining pore water will also be
314 decomposed into Ca^{2+} and OH^-. Step 3: Ca^{2+} and OH^- in lining pore water react with CO_2 again after
315 entering the drainage system, and $CaCO_3$ crystals are formed in the drainage pipeline.

316 (b) Mg^{2+} Mechanism of crystal blockage:

317 The crystallization mechanism of Mg^{2+} and Ca^{2+} is similar. In the first step: H_2O and CO_2 interact
318 with $MgCO_3$ in the surrounding rock, and the initial products are Mg^{2+} and HCO_3^-; in the second step:
319 Mg^{2+} and HCO_3^- react with $Mg(OH)_2$ in the lining, and gradually produce $MgCO_3$ and H_2O. At the same
320 time, part of $Mg(OH)_2$ in the lining pore water also decomposes into Mg^{2+} and OH^-; step 3: Mg^{2+} in lining
321 pore water reacts with CO_2 again after OH^- enters the drainage system and forms $MgCO_3$ crystal in a
322 drainage pipe.

(c) Al^{3+} Mechanism of crystal blockage:

The crystallization mechanism of Al^{3+} is different from Mg^{2+} and Ca^{2+}. The first step: In the surrounding rock, a part of Al^{3+} and OH^- in the water combine to form $Al(OH)_3$. In addition, because $Al(OH)_3$ is amphoteric hydroxide, another part of Al^{3+} and OH^- combine with AlO_2^- and H_2O. The second step: $Al(OH)_3$ reacts with OH^- in the lining to produce AlO_2^-. However, because the concrete can supplement Al^{3+} in the aqueous solution, the solubility of Al^{3+} increases, and then part of AlO_2^- reacts with Al^{3+} to produce $Al(OH)_3$, and the other part of Al^{3+} enters the drainage pipeline with the mixed solution. Step 3: Al^{3+} reacts with HCO_3^- in the drainage pipe to generate $Al(OH)_3$ and CO_2.

From the above analysis, it can be seen that the reaction principles of Ca^{2+}, Mg^{2+}, and Al^{3+} are relatively complex, but because the mixed solution is flowing, the time and space conditions of various chemical reactions are uncertain. For example, Al^{3+} and AlO_2^- are not co-existent in principle, but when their numbers do not match or the time of producing these two ions is inconsistent, the reaction cannot be carried out. However, as the mixed solution gathers into the drainage pipe, Al^{3+} and AlO_2^- form a consistent quantity, time, and space, and then a series of chemical reactions occur, resulting in drainage pipe blockage.

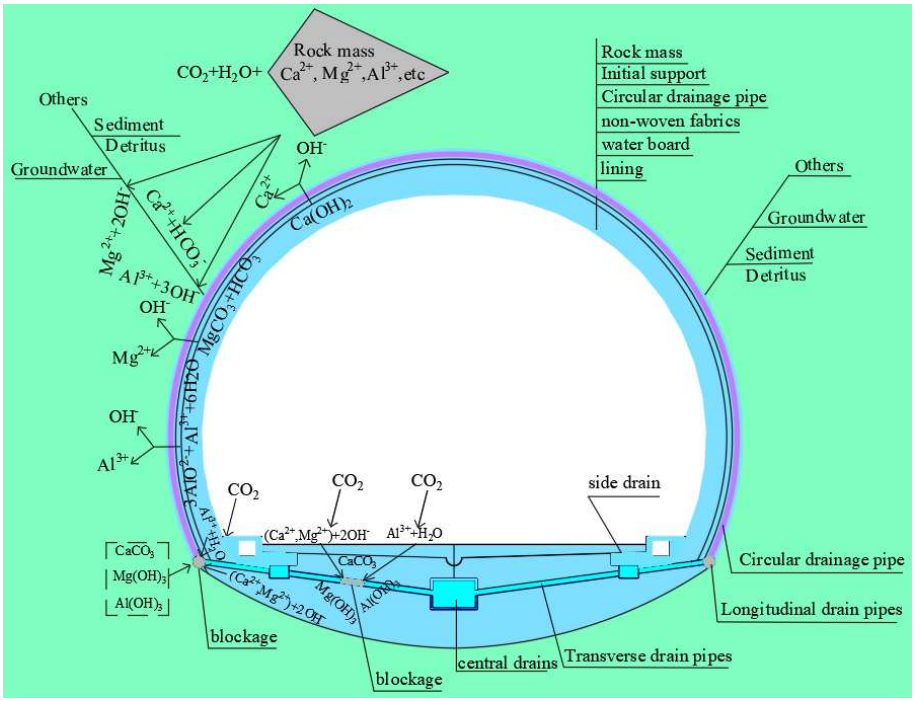

Fig 17 Reaction crystallization mechanism of mixed solution

It can be seen from Fig. 17 that the surrounding rock can provide the mixed solution of Al^{3+}, Ca^{2+}, Mg^{2+}, HCO_3^{2-} plasma. When the mixed solution in the rock mass passes through the lining, the lining can further supplement Al^{3+}, Ca^{2+}, Mg^{2+}+, and OH^- ions and generate AlO_2^-. At this time, there are some crystals in the pore water of the lining: $Mg(OH)_2$, $Ca(OH)_2$, and $Al(OH)_3$. Some of these crystals will adhere to the lining gap and pores, and the other part will be transferred to the drainage system by water. Due to the abundant CO_2 in the tunnel, the crystallization in the drainage pipeline is concentrated, and finally, the drainage pipeline is blocked.

5 Model test of drainage pipeline blockage

The source and mechanism of crystallization were analyzed through the above analysis. To further explore the formation law of crystallization in the drainage pipeline, the model experiment of drainage pipeline blockage was carried out. Several ions with a large concentration or influence on crystallization were selected to prepare solutions for indoor experimental research. The crystallization precipitation

blockage formed by ion reaction in tunnel drainage pipe was simulated, the content and change of crystallization were analyzed, the crystallization blockage law of pipeline was analyzed, and the crystal properties were explored, to provide a reference for preventing and controlling crystallization blockage in the tunnel.

5.1 Test scheme

Based on the drainage system design of the engineering tunnel, the test model is arranged. Combined with the results of water quality analysis in section 2 and component analysis in section 3, $CaCl_2$, $NaHCO_3$, $MgCl_2$, KCl, $AlCl_3$, and Na_2SO_4 solutions were prepared. During the experiment, the parts except for the outlet of the drainage pipe were sealed to prevent CO_2 from entering.

The working mechanism of the drainage system is as follows: put the pre-configured mixed solution into the high water tank 1 and the water tank 2 respectively, and then use the adjustable velocity valve to open the water valve according to the flow rate of 0.5 m / s. The mixed solution enters the low water tank 3 successively through the circular drainage pipe, longitudinal drain pipe, and transverse drain pipe, and then transfers the mixed solution to the high water tank by the pump until the cumulative time reaches 8 days.

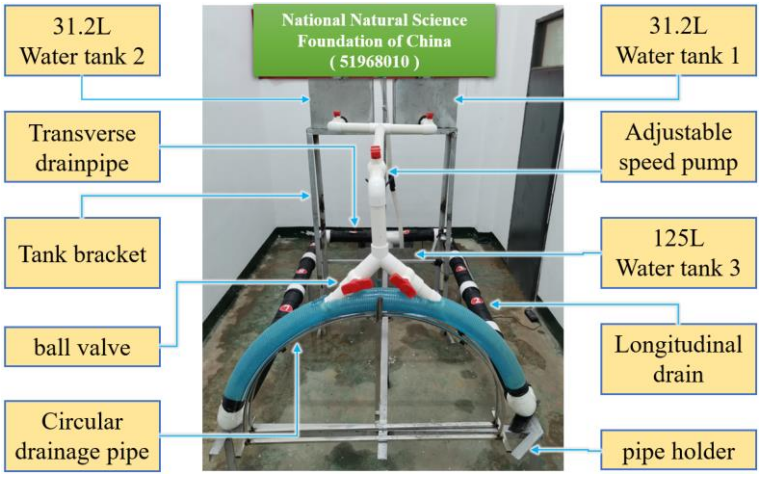

Fig. 18 Device Details Labeling

In Fig. 18, the longitudinal tube is a Φ110PE bellows with no grooves on the inner wall and is removable, and the length is 0.5 m. It is easy to dry after the test, and there is no gap in the middle of the assembly. The interface is sealed with waterproof adhesive tape, the length of the outer opening is 10 cm × 15 cm, and the spacing of the longitudinal tube is 1 m. The ring tube is a Φ75 spring hose with a length of 1.6 m. There are two grooves at both ends and PVC ball valves to control the water velocity at both ends of the circular drainage pipe.

(1) Strength of solution

Based on the above analysis results, 16 experiments were carried out according to different ion concentrations, and each experiment lasted for 8 days. The reagents were $CaCl_2$, $NaHCO_3$, $MgCl_2$, KCl, $AlCl_3$, and Na_2SO_4. Table 1 shows that there is a small amount of Fe^{3+}, Cu^{2+}, $Zn^{2+,}$ and Ba^{2+} ions in the tunnel drainage pipe, whose concentration is basically close to 0, and the influence on the crystal can be ignored. Therefore, the ion concentration higher than 0.00 mol/L is selected for the test. See Table 3, Table 4.

Table 3 The concentration of crystalline ions

Test	Concentration ratio of each ion/mol.L^{-1} $c(CO_3^{2-}):c(SO_4^{2-}):c(Ca^{2+}):c(Mg^{2+}):c(Al^{3+})$
Test.1	0.074:0.051:0.028:0.002:0.002
Test.2	0.074:0.053:0.082:0.006:0.011
Test.3	0.074:0.056:0.135:0.010:0.019
Test.4	0.074:0.058:0.189:0.014:0.028
Test.5	0.100:0.051:0.082:0.010:0.028

Test.6	0.100:0.0533:028:0.014:0.019
Test.7	0.100:0.056:0.189:0.002:0.011
Test.8	0.100:0.058:0.135:0.006:0.002
Test.9	0.126:0.051:0.135:0.014:0.011
Test.10	0.126:0.053:0.189:0.010:0.002
Test.11	0.126:0.056:0.028:0.006:0.028
Test.12	0.126:0.058:0.082:0.002:0.019
Test.13	0.152:0.051:0.189:0.006:0.019
Test.14	0.152:0.053:0.135:0.002:0.028
Test.15	0.152:0.055:0.082:0.014:0.002
Test.16	0.152:0.058:0.028:0.010:0.011

Table 4 Proportion of non-crystalline ions added /mol.L^{-1}

ionic types	$c(Cl^-)$	$c(K^+)$	$c(Na^+)$
content ranges	0.082～0.665	0.020～0.175	0.102～0.116
Content of each test	Calculation by actual dosage		
related explanations	This range is based on the actual addition of crystalline ions ion concentration conversion		

(2) Test Record and Analysis

To facilitate the follow-up analysis, longitudinal drain pipe, transverse drain pipe, and circular drainage pipe are marked as L, T, and C according to Fig. 19.

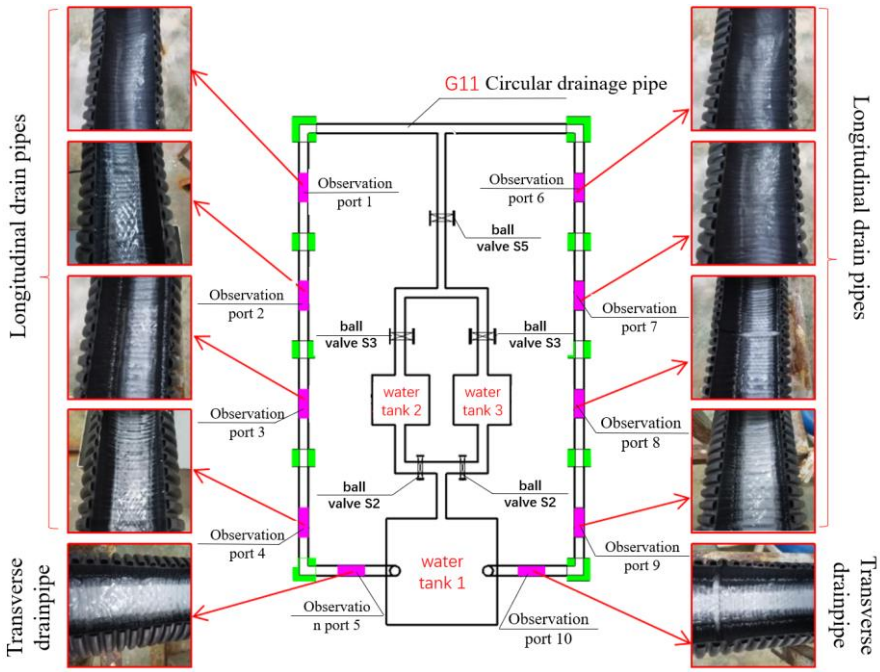

Fig. 19 Pipeline crystal growth

After each test, the drainage pipe was cut and the crystallization weight was recorded. The results are shown in Fig. 19. The crystallization weight of the drainage pipe in 16 tests was accumulated, and finally sorted out in Table 5:

Table 5 Crystallization record of mixed solution (unit: g)

Test \ Pipeline	L	T	C
T1	52.32	40.49	0.14
T2	57.35	44.93	0.2
T3	68.38	49.28	0.23
T4	72.52	51.05	0.22
T5	76.77	53.58	0.21
T6	81.67	56.05	0.22

T7	87.35	57.35	0.22
T8	89.92	60.05	0.2
T9	93.47	60.79	0.25
T10	92.34	59.81	0.21
T11	94.52	60.5	0.21
T12	96.64	61.12	0.19
T13	95.74	62.66	0.33
T14	96.3	61.38	0.26
T15	93.92	60.88	0.27
T16	96.44	64.63	0.35

Fig. 19 and Table 5 show that the amount of crystallization of longitudinal and transverse pipes is large, but the blockage of ring pipes is light. According to the crystallization weight, it can be inferred that for the actual tunnel, the blockage of longitudinal and transverse drainage pipes is more serious, and the degree of crystallization blockage of the circular drainage pipes is low.

5.2 Crystallization hazard analysis

According to the test results, the cumulative crystallization amount of each drainage pipe from Test.1 to Test.16 is used to measure the degree of crystallization blockage of the longitudinal drainage pipe, the transverse drainage pipe, and the circular drainage pipe, and it is converted to the cumulative crystallization amount of the pipeline per meter, and the blockage coefficient is introduced (the larger the blockage coefficient is, the more crystallization of the pipeline per meter is, the more serious the pipeline blockage is, and the greater the harm of pipeline clogging is). The definition is as follows:

$$\begin{cases} \alpha = \dfrac{\sum G_i}{G} \\ \gamma = \dfrac{\sum G_j}{G} \\ \beta = \dfrac{\sum G_k}{G} \end{cases} \qquad (20)$$

In Formula (20), α, γ, and β are the blockage coefficients of longitudinal drainage pipe, transverse drainage pipe, and the circular drainage pipe, respectively; G_i, G_j, and G_k are the cumulative crystallization amount of the longitudinal drainage pipe, transverse drainage pipe and circular drainage pipe per meter, g / m; g is the cumulative amount of crystallization of the whole drainage system per meter, and G = G_i+ G_j+ G_k, g / m.

After calculation, G_i, G_j and G_k are 21.056 g / m, 56.531 g / m and 0.145 g / m, respectively, and G = 77.702 g / m, so as to obtain:

$$\alpha = \frac{21.056}{77.702} = 0.271\ ; \quad \gamma = \frac{56.531}{77.702} = 0.728\ ; \quad \beta = = \frac{0.145}{77.702} = 0.002$$

Table 6 Crystallization conversion per meter pipeline

Type of pipeline	Cumulative crystallization amount /g	Length /m	Crystallization per meter pipeline /g.m^{-1}	Gross blockage factor
L	1345.65	64	21.056	α=0.271
T	904.5	16	56.531	γ=0.727
C	3.71	25.6	0.145	β=0.002

It can be seen from Table 6 that there is $\beta < \alpha < \gamma$: the transverse tube has more crystallization, the blockage coefficient γ is larger, the blockage degree is larger, and the crystallization hazard is higher, followed by the longitudinal tube. Because β = 0.002, it shows that $\beta \rightarrow 0$, the degree of crystallization plug is low, and the harm is small, that is, when the crystallization plugs, the ring tube is safer. The

relationship between crystallization and pipe blockage coefficient per meter is shown in Fig. 20.

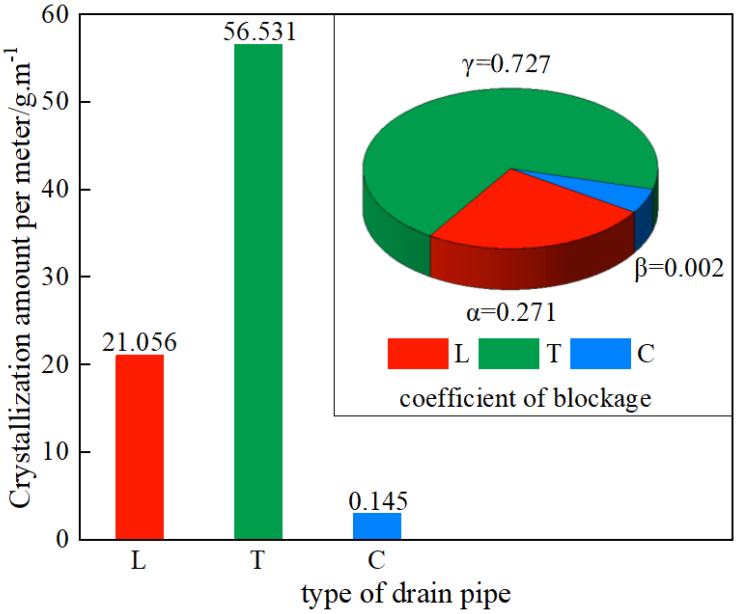

Fig 20 Crystallization and blockage coefficient per meter of pipeline

Fig. 20 shows that the crystallization amount per meter of the longitudinal drainage pipe is less than that of the transverse drainage pipe but higher than that of the circular drainage pipe, and the crystallization amount per meter of the ring tube is 0.145 g / m, indicating that the crystallization plug has little effect on the circular drainage pipe ; Fig. 20 shows that $\gamma \approx 2.7\alpha$, indicating that under the prescribed conditions, the amount of crystallization per meter of the transverse drainage pipe is about 2.7 times that of the longitudinal drainage pipe, and the degree of blockage is also high.

In summary, it is found that the blockage coefficient of the transverse pipe per meter is high and the amount of crystallization is large, which can be inferred that the crystallization in the drainage system has a great influence on the transverse drainage pipe. The possible reasons for the serious blockage of the horizontal pipe are as follows. (1) The horizontal drainage pipe is connected with the drainage ditch, and the sediment, precipitation, and crystallization in the vertical drainage pipe and the circular drainage pipe finally flow to the horizontal drainage pipe. When the drainage ditch is excluded, the horizontal pipe

may be seriously blocked due to poor drainage. (2) The transverse drainage pipe is connected with the drainage ditch, and contacts with the concrete lining layer at the outlet of the transverse pipe. The water contains some precipitation ions, such as SO_4^{2-}, CO_3^{2-}, etc., while the concrete lining contains Ca^{2+}, Mg^{2+} plasma. The concrete is eroded and crystallized to block the pipeline, which is consistent with the mechanism analysis of section 4.

6 Crystallization breaking experiment and design optimization

Through the analysis of sections 4 and 5, it is found that crystalline ions have a great influence on crystallization. Crystals from scratch, from less to more, adhere to the drainage pipe wall, and further ' grow ' over time, resulting in pipeline blockage. Through literature review, it is found that preventing crystal growth and breaking crystallization are effective measures for crystal removal. Given the effect of crystal removal and environmental protection, ultrasonic is proposed to remove crystals.

6.1 Crystallization breaking test

Through the model test, it can be seen that in Test.1, the internal crystallization of the drainage pipeline increases slowly with the increase of ion concentration. Therefore, the solution concentration in this chapter is studied by the solution ratio concentration in Section 5 Test.9. Ultrasonic is used to drive the vibration of the crystal around the pipe wall, resulting in the crystal falling off the pipeline and discharging along with the flow[29,30], to achieve the purpose of crystal removal. Therefore, a 35 ~ 60 kHz ultrasonic wave was used to crystallize the observation port 4 drainage pipeline with serious crystallization in Fig. 19.

6.1.1 Test principle and scheme

The ultrasonic principle is approximately regarded as a sine function curve, showing a certain

periodic change. When the crystal is broken by an ultrasonic vibration instrument, the main principle is that the crystal around the pipe wall is vibrated by ultrasonic, resulting in the crystal falling off from the drainage pipe wall, and finally discharged along with the flow[29,30].

Under the action of ultrasonic waves, the water produces bubbles of different sizes. When the bubble size reaches a certain degree, the water wave has a certain energy to collide with the crystal, which makes the crystal break down the drainage pipeline at the downstream discharge, and the crystal reacts to the bubble, resulting in the continuous generation of new bubbles, and reacts with the crystal again, to achieve the purpose of crystal removal, as shown in Fig. 21.

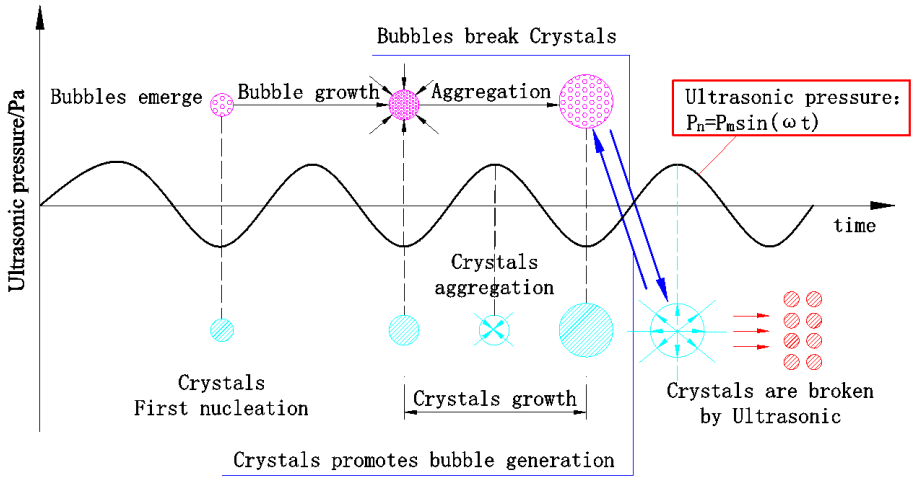

Fig. 21 The principle of breaking crystallization

Using this principle, based on section 4, group 9 experimental scheme, the crystallization breaking test is carried out. In each group of experiments, an ultrasonic vibration instrument was set at the observation port 4 drainage pipeline, and the crystal removal scheme is shown in Table 7. The crystallization process monitoring is shown in Fig. 22.

Table 7 The principle of breaking crystallization

Test	Ultrasonic frequency /kHz	Test cycle /24h	Monitoring of crystal breaking

			effect
Test.01	35		
Test.02	40		Photography, video recording and
		8	
Test.03	50		weighing
Test.05	60		

(a) Vibrator (b) Camera (c) Ultrasonic transmitter 35~60KHz

Fig. 22 Monitoring of crystal breaking process

6.1.2 Effect analysis

The crystal removal device was installed on the pipeline from day 1 to day 8 and was completely removed at noon every day for 8 consecutive days, as shown in Fig. 23.

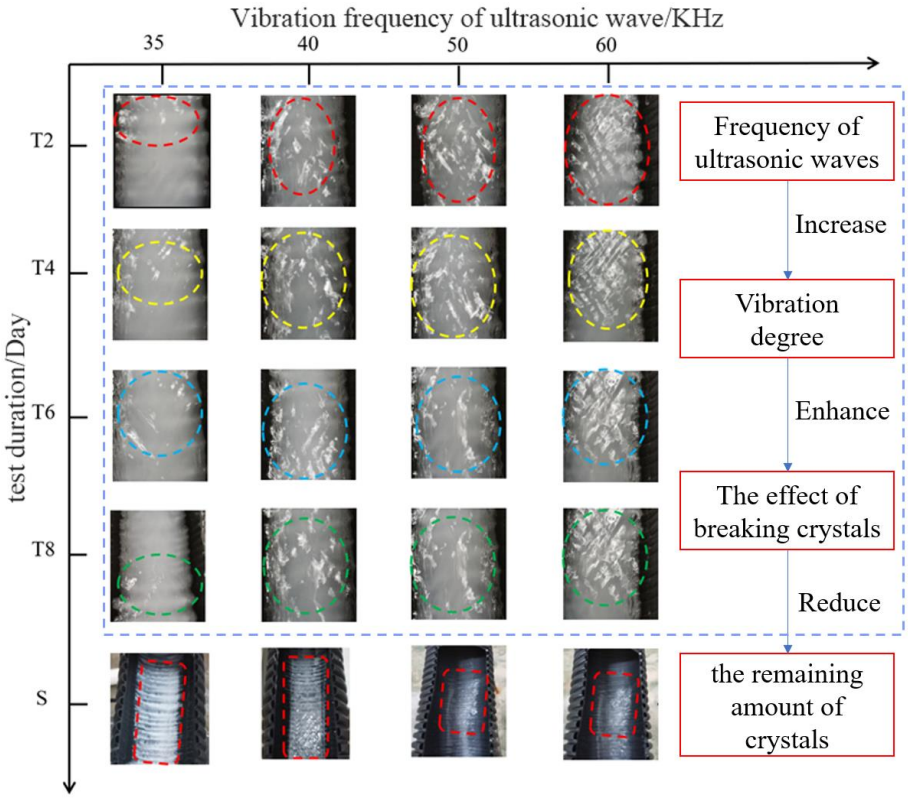

Fig. 23 Crystal breaking effect

In Fig. 23: T2 represents the second day of crystallization; t4 represents the fourth day of crystallization; 6 Represents the sixth day of crystallization; t8 represents the 8th day of breaking crystallization; s means that after the 8th day of crystallization, the residual amount of pipeline crystallization monitoring, the smaller the value, the better the effect of crystallization.

It can be seen that when using 35 kHz to break crystallization, with the increase of breaking time, the effect of crystal removal is certain, but the effect of crystal removal is not obvious. The effect of 40 kHz is more obvious than that of 35 kHz, and the amount of crystallization attached to the pipeline is less after 8 days. When 50 kHz is used to remove crystallization, the effect is more obvious. After 8 days, the crystallization of the pipeline is very little or even no; when 60 kHz is used to remove crystallization, the amount of crystallization attached to the pipeline is very small. Macroscopically, the effect is less different from that of 50 kHz.

According to the test records, the drainage pipes for 8 days were dried, and the quality differences of drainage pipes before and after crystallization were compared, to quantitatively deduce the effect of ultrasonic breaking crystallization. The comparative analysis of net weight before and after crystallization in the drainage pipes is shown in Fig. 24.

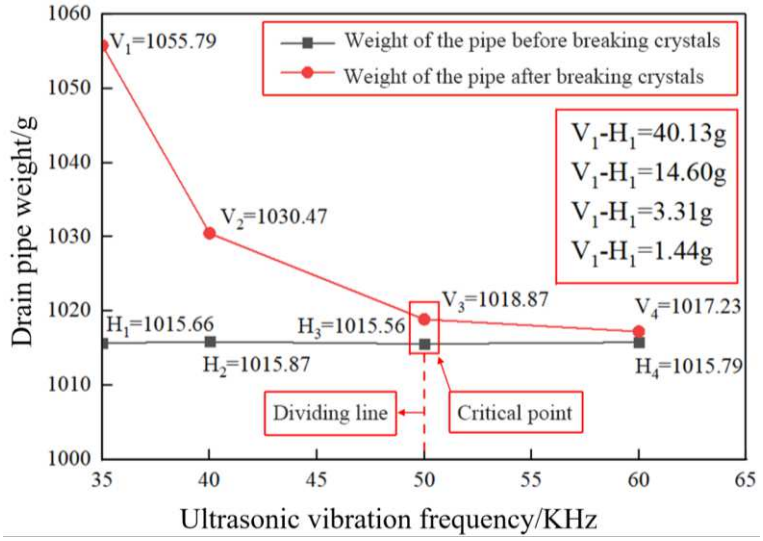

Fig. 24 Variation of pipe net weight difference

The ultrasonic crystal removal effect is obvious. It is found in Fig. 23 and Fig. 24 that the crystal removal effect at 50 kHz is not significantly different from that at more than 50 kHz. The reason may be as follows:

（1）Both sides of the drainage pipeline hinder the ultrasonic wave, and the ultrasonic wave only plays a role in a certain range. Beyond this range, even if the frequency is increased, the crystal breaking effect is similar. As shown in Fig. 25, the range of 50 kHz and 60 kHz is similar, and the range of crystallization is similar, which may be mainly related to the role of the drainage pipe wall, that is, the ultrasonic propagation process is blocked by the pipe wall, resulting in the propagation blocked.

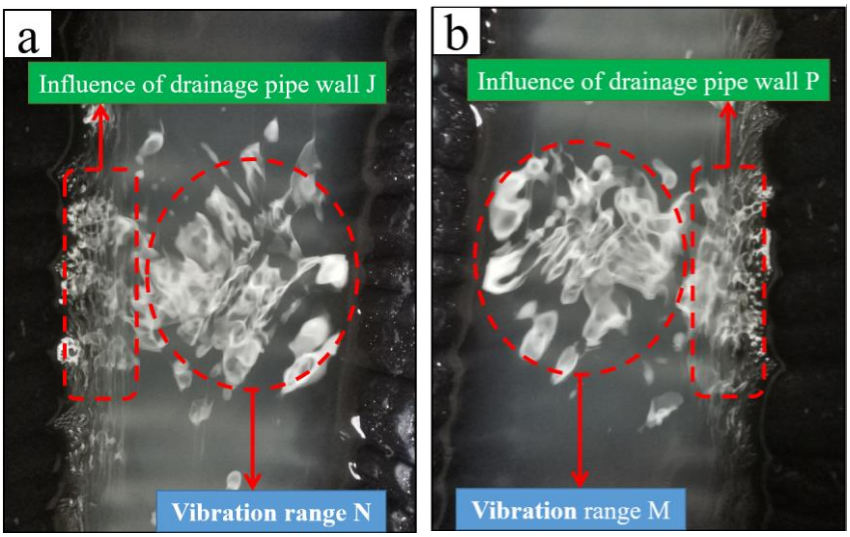

(a) Ultrasonic vibration frequency is 50KHz

(b) Ultrasonic vibration frequency is 60KHz

Fig. 25 Ultrasonic action

（2）Ultrasonic wave is also a kind of sound wave, and its propagation path is related to the medium, where the medium is mainly the solution formed by the mixing of various ions, the precipitation produced by the reaction between ions, the wall of the drainage pipe, the diameter of the drainage pipe, etc., which will affect the propagation of the sound wave, and then cause the ultrasonic vibration to be within a certain range. Even if the frequency is increased, the effect is not significantly different.

In summary, it is found that the greater the acoustic frequency is, the more obvious the effect of crystallization is. The less the residual crystallization of the drainage pipeline after the removal is, and the longer the time is, the more obvious the crystallization is. The self-weight statistics of the drainage pipeline before and after the crystallization are shown in Fig. 24. The crystallization of ultrasonic waves is better and more obvious, and with the increase of ultrasonic frequency, the effect of crystallization is more obvious. When the vibration frequency is about 50 kHz, the crystal adhesion of the drainage wall tends to be flat. Therefore, at normal temperature and flow rate, it is recommended that a 50 kHz

ultrasonic frequency should be used to break the crystal. Therefore, the ultrasonic frequency based on this parameter will be used as the ultrasonic frequency for breaking the crystal.

6.2 Optimal design of drainage system

The research group has shown that the following countermeasures are proposed to solve the problems of reverse drainage and insufficient drainage when the drainage pipe is blocked[1]: connecting longitudinal drainage pipe. Longitudinal drainage pipe between transverse drainage pipe and circular drainage pipe uplifted upward, showing a ‘ V ’ shape, as shown in Fig. 26. According to the existing drainage method, when the water flow through the longitudinal drainage pipe is large, the ‘ V ’ shaped longitudinal drainage pipe scheme can effectively share the drainage, avoid the problems of reverse drainage and insufficient drainage of the drainage pipe, and also improve the pipeline flow smoothness and reduce the crystal blockage of the drainage pipe.

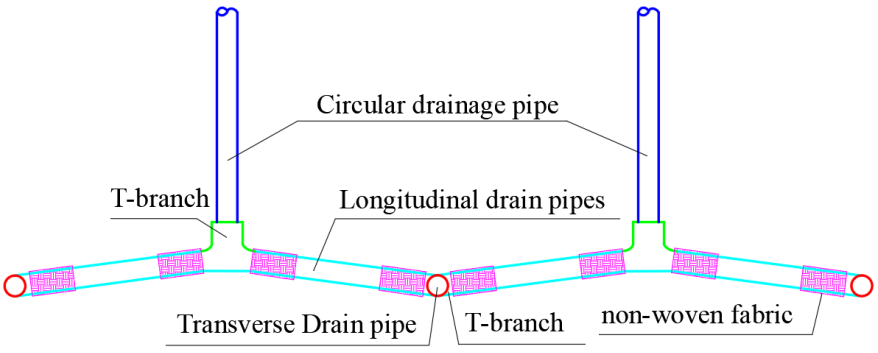

Fig. 26 ‘V’ shape drainage arrangement

Through the above analysis, it can be seen that the blockage of the drainage pipe is related to the type of ions, and there is a stable crystallization and growth area. According to the test in section 5, it is known that the crystallization amount of the transverse drainage pipe is more. Therefore, based on Nie's research results[1], it is suggested that when optimizing the crystal removal of the drainage system, the crystal removal device can be installed at the midpoint of the transverse drainage pipe, which can

effectively remove the crystal, and then the crystal is discharged with the water flowing to the drainage ditch.

Optimizations are shown in Fig. 27 and Fig. 28.

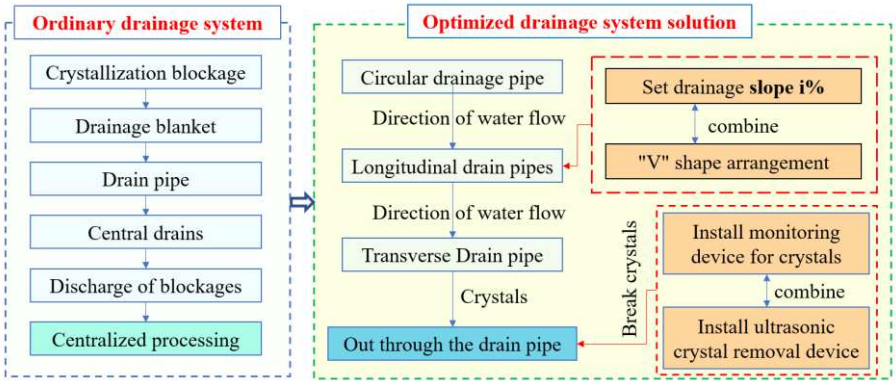

Fig. 27 Optimization process

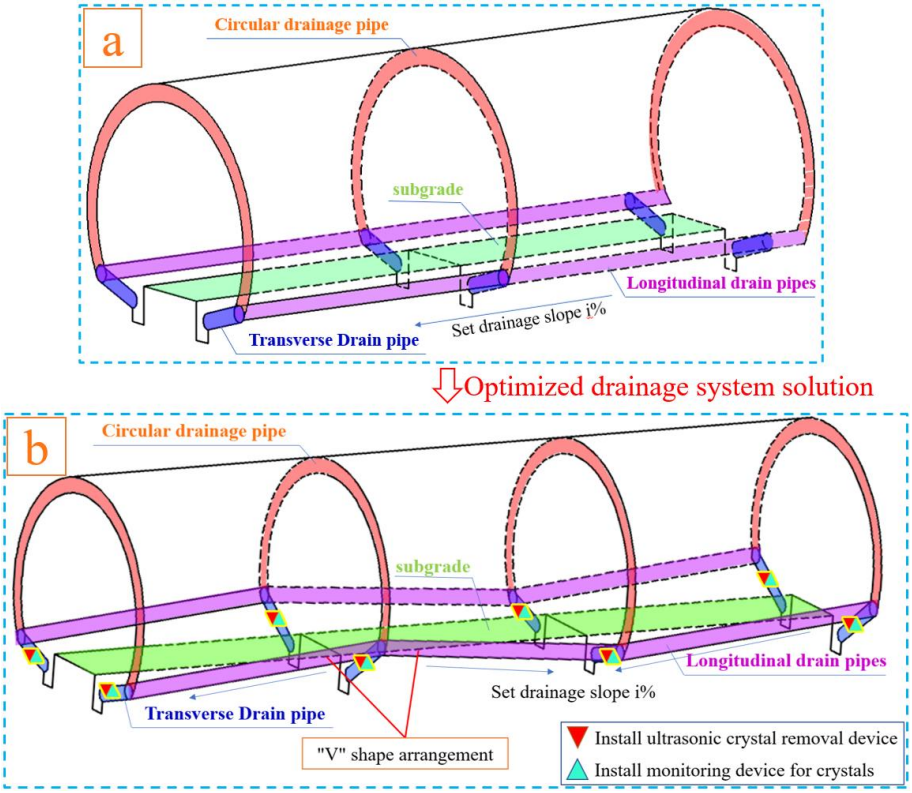

Fig. 28 Optimization design of drainage system

Fig. 28 shows that: In the optimized crystallization removal system, the intelligent monitoring crystallization system is installed at the midpoint of each section of the transverse drainage pipe. The

crystallization of the drainage system can be observed in real-time by the crystallization monitoring system, and then the ultrasonic crystal removal device is opened/closed to select the time of removal in real-time.

7 Conclusion

(1) Through the field investigation of the dolomite tunnel, the crystals formed in the drainage pipeline system are mainly $CaCO_3$, $Mg(OH)_2$, $Al(OH)_3$, and other forms, and the mass fraction and concentration of Ca^{2+}, Mg^{2+}, Al^{3+}, SO_4^{2-}, OH^- are higher, and other ions are less ;

(2) Through the study of pipeline crystallization blockage mechanism, it is found that the formation process of crystals is complex, and there are many factors affecting the crystallization blockage. This paper mainly focuses on the mechanism of Ca^{2+}, Mg^{2+}, and Al^{3+} plasma blockage, that is, the crystallization blockage mechanism of mixed solution. The main crystallization components are $CaCO_3$, $Mg(OH)_2$, $MgCO_3$, $Al(OH)_3$, etc.

(3) The indoor model test was used to simulate the crystallization blockage of the drainage pipe, and it was found that the crystallization blockage of the drainage pipe mainly occurred in the longitudinal drainage pipes and transverse drainage pipes, and the crystallization amount of circular drainage pipe was very small. The blockage coefficients of the longitudinal drainage pipe, the transverse drainage pipe, and the circular drainage pipe are α, γ, and β, respectively, and $\boldsymbol{\alpha} = 0.271$, $\boldsymbol{\gamma} = 0.728$, and $\boldsymbol{\beta} = 0.002$, respectively. There is $\boldsymbol{\beta} < \boldsymbol{\alpha} < \boldsymbol{\gamma}$, indicating that the crystallization blockage has a great influence on the transverse drainage pipe. The transverse drainage pipe per meter has more crystallization, a higher plugging degree, and stronger harmfulness.

(4) Ultrasonic wave has an obvious effect on crystal removal, and the adhesion of crystal drainage pipe wall decreases with the increase of frequency. Through the comparison of vibration frequencies

from 35 kHz to 60 kHz, it is found that when the vibration frequency is about 50 kHz, the crystal removal effect is obvious, and when the vibration frequency exceeds this, the crystal removal effect is not significantly different. Therefore, 50 kHz is recommended as the ultrasonic crystal removal frequency.

CRediT authorship contribution statement

Junying Rao: conceptualization, methodology, investigation, test methods, writing-review, funding; Yanghao Xue: data curation, test design, test operation, writing-first draft-review and editing; Yonghu Tao: test supervision, data analysis and optimization, Writing - first draft - review and editing.

Declaration of Competing Interest

The authors declare no competing interests.

Acknowledgments

This study was sponsored by the National Science Foundation of China (Grant Nos. 51968010 and 51608141).

Data availability

The data that supports the findings of this study are available from the corresponding author upon reasonable request.

References

[1] Chongxin Nie. Influence Of Pipe and Pipe Connection Form on Crystallization Of Drainage System in Dolomite Tunnel [D]. Guizhou: Guizhou University (2021).

[2] Yifan Chen, Yujun Cui, Antoine Guimond Barrett, Francesco Chille, Sylvain Lassalle. Investigation of calcite precipitation in the drainage system of railway tunnels[J]. Tunnelling and Underground

Space Technology, **84**: 45-55(2019).

[3] Chunjun GAO, Lihui Xiang, Xuefu Zhang, Yuanfu Zhou, Shiyang Liu. Lining stress caused by crystal lization clogging of tunnel drainage pipe at different water levels[J]. Journal of Chongqing Jiaotong University (Natural Science), **38**(05): 45(2019).

[4] Jun-Ying R, He-Lin F, Quan Y, Wen-Bo L. Fuzzy evaluation model for karst highway tunnel safety. Electronic Journal of Geotechnical Engineering, **18**, 5173-5184(2013).

[5] Jiaqi Guo, Jianxun Chen, Fan CHEN, Yanbin Luo, Qin Liu. Water Inrush Criterion and Catastrophe Process of a Karst Tunnel Face with Non-persistent Joints [J]. China Journal of Highway and Transport, **31**(10): 118-129(2018).

[6] Junying Rao. Analytical Solutions And Application For Stress Around deeply Buried Holes In Karst With Elastic Theory[J]. Chinese Journal of Rock Mechanics and Engineering, 2015, 34(6): 1296.

[7] Meng Tao. Study on characteristics of dolomite in well Xike 1 of Xisha Islands [D]. Shandong: China University of Petroleum(2019).

[8] Caijin Xie, Junying Rao, Kailiang Nie, Zhongyong Liang, Ning Liu, Xia Zhao, Dengkai Liu. Study on the Electron Microscope Scanning Experiment and Damage of Muddy Dolomite in Guiyang [J]. Construction Technology, **47**(S1): 1-7(2018).

[9] Rao Junying, Tao Yonghu, Xiong Peng, Nie Chongxin, Peng Hao, Xue Yanghao, Xi Zuowei, Lei Mingfeng. Research on the Large Deformation Prediction Model and Supporting Measures of Soft Rock Tunnel[J]. Advances in Civil Engineering,**2020**(2020).

[10] Xiaoxiong Guo. Crystallization Mechanism and Countermeasures of Drainage System for Railway Tunnel [J]. China Railway Science, **41**(01): 71-77(2020).

[11] Stefanie Eichinger, Ronny Boch, Albrecht Leis, Günther Koraimann, Cyrill Grengg, Gunnar Domberger, Manfred Nachtnebel, Christian Schwab, Martin Dietzel. Scale deposits in tunnel

609 drainage systems–A study on fabrics and formation mechanisms[J]. Science of the Total
610 Environment,**718**(C) (2020).
611 [12] Yian Zhang. Study on Crystalline Pipe Blocking Mechanism and Tunnel Structure of Emei to
612 Hanyuan High Speed Tunnel Drainage System [D]. Sichuan: Chongqing Jiaotong University(2021).
613 [13] Pezzuto A , Sarver E . A lab study of mineral scale buildup on line and traditional PE water pipes
614 for acid mine drainage[J]. Journal of Sustainable Mining(2020).
615 [14] Gaojin Liu, Guangze Zhang, Tao Feng. Exploration on the Causes of Erosion about Tunnel through
616 Different Saliferous Strata [J]. Journal of Railway Engineering Society, **35**(10): 15-19(2018).
617 [15] Yonghu Tao, Junying Rao, Peng Xiong, Chongxin Nie, Caijin Xie. Operating tunnel prototype-
618 model lining stress theory model and application [J]. Journal of Xi'an University of Technology,
619 **37**(03): 423-432(2021).
620 [16] Eichinger S, Boch R, Hippler D, Egartner I, Orieschnig A, Leis A, Dietzel M. Carbonate precipitates
621 impairing drainages in an Austrian motorway tunnel-Investigation on growth dynamics and
622 environmental dependencies[J]. In EGU General Assembly Conference Abstracts, **35**(04): 132-
623 141(2018).
624 [17] Girmscheid G, GARMISCH T, Meinlschmidt A. Versinterung von Tunneldrainagen-Empfehlungen
625 fuer die Instandhaltung von Tunneln/Scale sintering in tunnel drainages-recommendations for
626 maintenance of tunnels[J]. Bauingenieur, **78**(12) (2003).
627 [18] Xuefu Zhang, Yuanfu Zhou, Bin Zhang, Yuanjiang Zhou, Shiyang Liu. Investigation and Analysis
628 on Crystallization of Tunnel Drainage Pipes in Chongqing[J]. Civil Construction, 2018(2019).
629 [19] Fei Ye, Chongming Tian, Meng Zhao, Biao He, Jian Wang, Han Xin. The disease of scaling and
630 cloging in the drainage pipes of a tunnel under construction in Yunnan[J]. China Civil Engineering

631 Journal, **53**(S1): 336-341(2020).

632 [20] Jung HS, Han YS, Chung SR, Chun BS, Lee YJ. Evaluation of advanced drainage treatment for old
633 tunnel drainage system in Korea[J]. Tunnelling and Underground Space Technology, **38**(3): 476-
634 486(2013).

635 [21] Park EH, Nam JW, Han YS, Kim HG, Chun BS. An evaluation of treatment technologies for anti-
636 scale in drainage works using simulation test of road tunnel[J]. The Macmillan Company, **29**(07):
637 1229-2427(2013).

638 [22] Liu SY, Gao F, Zhang XF, Han FL, Zhou YF, Xiang K, Xiao DJ. Experimental study on anti-
639 crystallization law of tunnel transverse flocking drainpipe at different velocities[J]. Asia-Pacific
640 Journal of Chemical Engineering(2020).

641 [23] Zhou Chou. Study on The Plug of The Tunnel Drainage Pipe Mechanism caused by Groundwater
642 Seepage Crystallization in Karst Area and The Proposal of Treatment [D]. Changan：Chang'an
643 University(2015).

644 [24] Jianhua Cao, Daoxian Yuan, Genxing Pan. Preliminary Study on Biological Action in Karst
645 Dynamic System [J]. Earth Science Frontiers, **8**(1): 203-208(2001).

646 [25] Lian Bin, Daoxian Yuan, Zaihua Liu. Effect of microbes on karstification in karst ecosystems [J].
647 Chinese Science Bulletin, **56**(26): 2158-2161(2011).

648 [26] Jiwu Huang, Zhou Li. X - ray Diffraction - Test Principle, Method and Application of
649 Polycrystalline Materials [M]. Beijing: Metallurgical Industry Press(2012).

650 [27] Datong Zhang, Goldstein,J.I. Scanning Electron Microscopy and X - ray Microanalysis [M]. Beijing:
651 Science Press(1988).

652 [28] Zhifen Li. Modeling, Optimization and Control of Continuous Crystallization Process [D]. Liaoning：

653 Dalian University of Technology(2018).

654 [29] Alain L, Marc D. Ultrasonic Wave Propagation in Non Homogeneous Media[M]. Springer Berlin

655 Heidelberg(2008).

656 [30] Bingchen Jiang. Study On Ultrasonic Anti Scaling Technology Of Crude Oil Pipeline Cleaning [D].

657 Haerbin: Harbin Institute of Technology(2016).

658 [31] Zhou Chou. Study on The Plug of The Tunnel Drainage Pipe Mechanism caused by Groundwater

659 Seepage Crystallization in Karst Area and The Proposal of Treatment [D]. Changan: Chang'an

660 University(2015).

661